

## Mapping Land Surface Temperature and Land Cover to Detect Urban Heat Island Effect: A Case Study of Tarkwa, South West Ghana

Michael Soakodan Aduah, Saviour Mantey and Naa Dedei Tagoe  
Department of Geomatics Engineering, University of Mines and Technology,  
P.O. Box 237, Tarkwa, Ghana

**Abstract:** Urban Heat Island (UHI) effect controls internal climates of buildings and affects energy use and comfort of urban dwellers. The objective of this study was to detect UHI from Land Surface Temperature (LST) and to investigate whether land cover has any influence on UHI in Tarkwa, South West Ghana using satellite remote sensing techniques. A Landsat 7 ETM+ image, DEM and meteorological data were used to generate a land cover map with the maximum likelihood classification algorithm while LST was modeled with the Landsat Plank's curve. Validation of the LST map was achieved by comparing it with air temperature measured at the UMaT meteorological station. The mean modeled LST of 298.60 Kelvin compared well with the mean observed air temperature of 298.30 Kelvin. Furthermore, LST ranged between 289 and 305 Kelvin while urban areas and bare soils had higher LSTs than vegetated areas implying that higher NDVI areas are associated with lower temperatures. Hence, LST maps produced indicated the existence of UHI effect in the Tarkwa area. From the study it is evident that impervious and non-evaporative surfaces have high LSTs due to absence of vegetation. Therefore, uncontrolled land cover changes may intensify the UHI effect. The study has proven that remote sensing can be used in operational mapping of LST for climate studies, vegetation monitoring and detecting UHIs in the humid regions of Ghana. This confirms the important role Earth observation and geo-information technology can play in environmental monitoring and management as global climate and land cover changes.

**Key words:** Geo-information, land cover, landsat, LST, remote sensing, urban heat island

### INTRODUCTION

Urban Heat Island effect (UHI) is a phenomenon that results in higher temperatures in urban areas than the surrounding rural areas (Jensen, 2000). The phenomenon is influenced primarily by amount of vegetation and water pervious surfaces. There is therefore less evaporation in urban areas to reduce land surface temperatures due to the replacement of vegetation and water pervious surface by impervious surfaces. These surfaces together absorb heat energy resulting in higher air temperatures in urban areas. UHI effect is an important climatic phenomenon to study because local temperatures influence the microclimate through processes such as moisture retention, vegetation growth and levels of atmospheric and plant evaporation. Also excessive heat in the urban area can cause a variety of problems including skin cancer and higher energy bills due to the need for air conditioners.

To mitigate UHI there is the need to determine the levels of air temperature in urban areas through time. Regulations can then be developed to reduce the overall heat budget. Some of the regulations can be:

- Providing incentives for house owners to grow lawns, trees and gardens
- Development of recreational and green areas
- Promoting the use of the right building materials

Over the centuries devices have been built to measure air temperature with reliable accuracies. However, the measurement has been constrained to laboratories, climate stations and eddy covariance flux towers. It is evident from past studies that temperature varies with landscape type, elevation and latitude (Yuan and Bauer, 2007; Gluch *et al.*, 2006; Small, 2006). For instance, temperatures in mountainous areas are lower than those in the surrounding valleys and floodplains within the same catchment. Since the urban environment is spectrally complex and not homogeneous, Land Surface Temperature (LST) measurement at point locations is not representative enough. Spatially distributed measurement is therefore the most reliable approach to provide complete spatial coverage for monitoring UHIs. However, due to high cost of acquisition, installation and maintenance of climate equipment, it is often impossible to measure enough LSTs

at point locations so as to achieve complete spatial coverage. Because of these shortcomings, ground methods of measuring temperature are inadequate for large areas. In contrast, thermal remote sensing techniques provide continuous spatial coverage over large areas and it is possible to measure repeatedly over a long period of time. Thermal remote sensing methods have become reliable over the years with development of new sensors and techniques. Many studies have been carried out with success (Yuan and Bauer, 2007; Gluch *et al.*, 2006; Small, 2006; Kato and Yamaguchi, 2005; Sobrino *et al.*, 2004). The remote sensing methods (Sobrino *et al.*, 2004; Jensen, 2000) use the thermal inertia of land surface materials and apply physical models to generate LSTs. Each satellite system has its own calibrated heat measurement parameters associated the thermal bands. Satellite methods in LST mapping have the potential to provide complete data needed for detecting and monitoring UHI effect since data is provided for every grid cell within the study area. In this study, the Landsat Plunk's curve was used to model LST of Tarkwa and its surrounding areas to detect UHI effect and to determine its relationship with land cover. The study was carried out in April 2011 as part of efforts to evaluate methods for monitoring the environment of Tarkwa mining area in Ghana.

## MATERIALS AND METHODS

**Study area:** Tarkwa is located about 89 km north of Takoradi, the Western regional capital of Ghana, on latitude 5° North and longitude 2° West. The study area is characterized by dense forests and large rubber plantations in the south. The eastern, northern and north western part of the study area is dominated by large scale mining activities. Apart from large scale surface mining, small scale mining is also practiced. Subsistence farming is also practiced by some villages around Tarkwa, especially those that do not fall within the mining concessions. The Bonsa River is the main source of water within the study area and it joins the Ankobra River in the west. Tarkwa is a humid tropical environment with heavy rainfall throughout most of the year. The study area is currently experiencing land cover changes and floods due to a plethora of human activities. In Fig. 1 a map of Ghana is displayed showing the location of the study area.

**Data acquisition:** Data for the study included a Landsat 7 Enhanced Thematic Mapper plus (ETM+) image captured on January 15 2002. In addition, a digital elevation model derived from the Shuttle Radar Topography Mission (SRTM DEM) was acquired. Also air temperature data was obtained from the University of Mines and Technology (UMaT) meteorological station,

Tarkwa, Ghana in April 2011. The Landsat 7 ETM+ image was used because:

- It was available at no cost.
- Many studies have documented successful mapping of urban heat island effect using images from this sensor.
- The image has a high spatial resolution making it possible to detect small land surface features and processes.

The satellite image and the SRTM DEM were ordered and downloaded from the United States Geological Survey (USGS) Websites in April 2011.

### Image processing:

**Geo-referencing:** Geo-referencing is executed to allocate real world coordinates to a satellite image. It is also done to register satellite images and other maps (e.g., topographic and land use maps) to a common projection and datum. The satellite image used in this study was already geo-referenced and orthorectified with the Universal Transverse Mercator projection zone 30 North (UTM 30N) by USGS, therefore it was not geo-referenced. The SRTM DEM was re-projected to the UTM Zone 30N so as to align properly with the rest of the data. However, since the study area is smaller than the scenes, the analysis was based on a subset of the image and the SRTM DEM.

**Atmospheric correction:** Pre-processing of satellite data is necessary to correct for errors in the measured reflectance due to alteration of the electromagnetic radiation as it passes through the atmosphere (Lunetta and Elvidge, 1999). The raw satellite image was pre-processed before image interpretation. This is because the atmospheric contribution to the recorded signals and sensor errors can lead to inaccurate image interpretation (Coppin *et al.*, 2004). The atmospheric correction was carried out in two stages. Firstly, haze was removed from the visible and near-infrared bands. Secondly, the thermal band, band 62 was atmospherically corrected by applying the online MODTRAN algorithm developed by the National Aeronautics and Space Administration (NASA) of the United States. This algorithm is online and available at <http://atmcorr.gsfc.nasa.gov/>. The algorithm was used to compute downwelling irradiance, atmospheric transmittance and upwelling radiances; parameters needed to compute surface leaving radiance,  $L_T$ .

**Image classification:** Image classification is one of the most important parts of digital image processing. Often, the maps produced from classification serve as input to other algorithms for further analysis. The spectral pattern

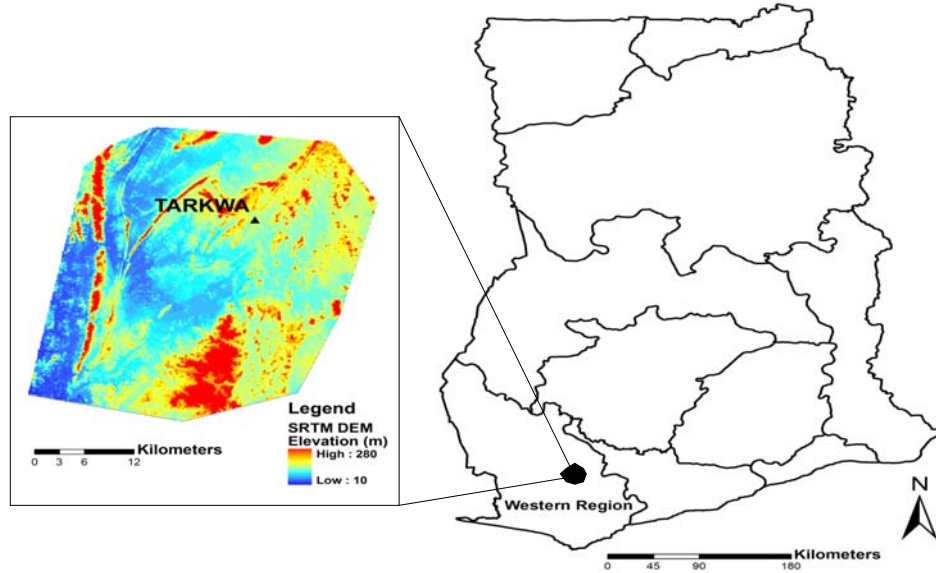


Fig. 1: Map of Ghana showing the study area

within the remotely sensed image is the basis for classification (Lillesand and Kiefer, 1994). A land cover map with five classes; bare soil, urban, dense forest, open forest/farm and water was generated by classifying a composite of the non-thermal bands (i.e., bands 1, 2, 3, 4, 5 and 7) using the maximum likelihood algorithm (Jensen, 2000). Training signatures were selected based on unsupervised classification and local knowledge of study area. However, accuracy assessment of land cover map was not carried out since ground truth data at time of satellite overpass was not available.

**Land surface emissivity and normalized difference vegetation index:** Normalized Difference Vegetation Index (NDVI) and land surface emissivity ( $\epsilon$ ) are required to compute LST when using the Landsat Plank's curve. Therefore NDVI was computed from the near-infrared (band 4) and red (band 3) bands of the Landsat7 ETM+ image using Eq. (1). Emissivity is the ratio of the radiant energy emitted from a real world body to that emitted by a black body at the same temperature (Jensen, 2000). Land surface emissivity varies for different materials depending on their ability to absorb heat energy (Table 1). According to Sobrino *et al.* (2004), there is a relationship between NDVI and land surface emissivity. The relations developed by Sobrino *et al.* (2004) were therefore combined and used to calculate land surface emissivity (Eq. 2).

$$NADV = \frac{band4 - band3}{band4 + band3} \quad (1)$$

Table 1: Emissivity of land covers in study area

Land cover	$\epsilon$
Urban (Mostly oxidized steel)	0.76
Dense forest	0.98
Open forest/Farm	0.96
Bare soil	0.96

$$\epsilon = 0.004 \left[ \frac{NDVI - NDVI_{min}}{NDVI_{max} - NDVI_{min}} \right]^2 + 0.986 \quad (2)$$

where,  $NDVI_{max}$  and  $NDVI_{min}$  are the maximum and minimum NDVI for the study area.

**Land Surface Temperature:** LST was calculated using the ETM+ band 62 (i.e., the low gain thermal band). The thermal band detectors record top of atmosphere brightness temperature (TOA) in the form of Digital Numbers (DN). Therefore, by using the single channel algorithm (Yuan and Bauer, 2007; Sobrino *et al.*, 2004) the TOA can be converted to surface temperatures. According to Yuan and Bauer (2007), surface temperatures obtained with this model are highly accurate. The errors are less than 2 Kelvin. In this study TOA was computed with Eq. (3):

$$L\lambda = \frac{L_{max} - L_{min}}{QCAL_{max} - QCAL_{min}} (DN - QCAL_{min}) + L_{min} \quad (3)$$

where,  $L\lambda$  is TOA radiance at the sensor's aperture ( $W/m^2 \text{ sr } \mu m$ ),  $QCAL_{max}$  and  $QCAL_{min}$  are the highest and the lowest range of re-scaled radiances, DNs are the image radiances,  $L_{min}$  and  $L_{max}$  are the TOA radiances that

are scaled to  $QCAL_{min}$  and  $QCAL_{max}$  in  $W/m^2 sr \mu m$ . These parameters are located in the Meta file of the satellite image. The surface leaving radiance  $L_T$  was then computed with parameters obtained from the MODTRAN atmospheric correction algorithm using Eq. (4).

$$L_T = \frac{L\lambda - L\mu - \tau(1 - \epsilon)Ld}{\epsilon} \quad (4)$$

where,  $L\mu$  is the upwelling radiance,  $Ld$  is the downwelling radiance,  $\tau$  is the atmospheric transmission and  $\epsilon$  is the emissivity of the surface. Radiances are in units of  $W/(m^2 sr \mu m)$  while the transmission and the emissivity are unit less.

Finally, LST was calculated using the Landsat Planck's curve (Eq. 5) for determining surface temperature (Yuan and Bauer, 2007; Kerle *et al.*, 2004; Gratton *et al.*, 1993):

$$T = \frac{K^2}{\ln\left[\frac{K1}{LT} + 1\right]} \quad (5)$$

where, T is the LST in Kelvin, for Landsat 7 ETM+;  $k1 = 666.09 W/m^2sr$  and  $k^2 = 1282.71 K$  and  $L_T$  is surface leaving radiance.

## RESULTS AND DISCUSSION

The results of the study are shown in Fig. 2, 3, 4, 5 and Table 2 and 3. It can be observed from Fig. 2 that the major land covers in the study area are dense forests, open forests, bare soil (result of surface mining) and urban areas. The forest class dominates the landscape while the water class constitutes the smallest land cover. The LST for the study area ranged between 289 Kelvin and 305 Kelvin. The average LST of the land covers are presented in Table 2. The urban surfaces had the highest and forest

Table 2: LST and Land cover

Land cover	Min LST (K)	Max LST (K)	Average LST (K)	SD (K)
Bare soil	291.53	298.25	294.68	1.90
Urban	292.34	297.80	294.24	1.37
Open forest	292.32	295.30	293.73	0.66
Dense forest	291.91	294.90	293.37	0.96
Water	291.97	297.02	293.48	1.46

Table 3: NDVI per Land cover

Land cover	Min NDVI	Max NDVI	Average NDVI	SD
Bare soil	0.11	0.24	0.15	0.03
Urban	0.15	0.32	0.22	0.05
Open forest	0.29	0.38	0.32	0.02
Dense forest	0.23	0.29	0.26	0.02
Water	0.07	0.20	0.14	0.03

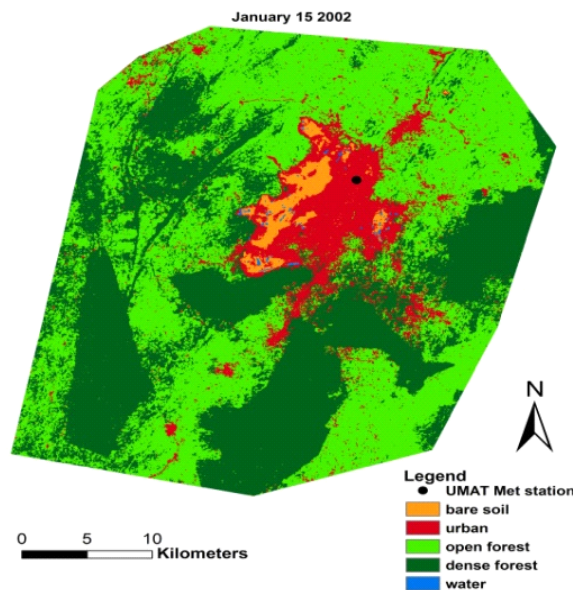


Fig. 2: Land cover map

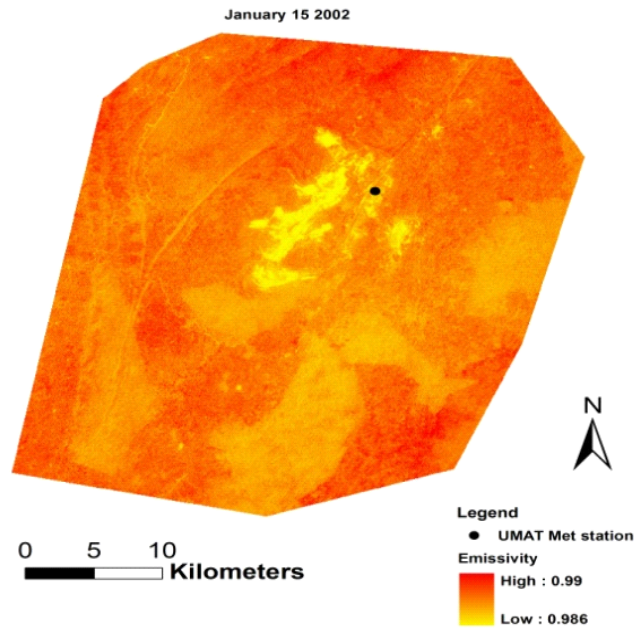


Fig. 3: Emissivity map

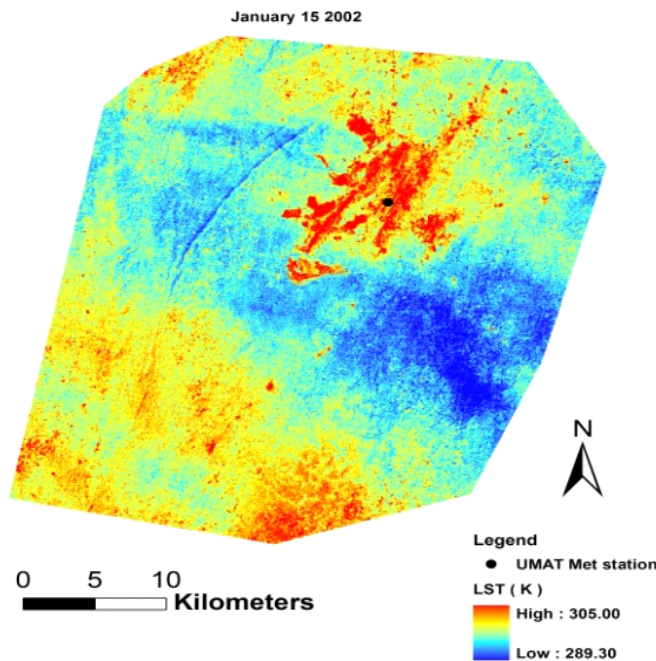


Fig. 4: LST map

areas, the lowest LSTs (Fig. 4, 6 and Table 2). This is due to the lowest and highest emissivity of urbanized and vegetated environments, respectively (Fig. 3). Also bare soil, a significant land cover both within urban areas and the mining areas has an average LST lower than only that of the urban surfaces. This suggests that, high NDVI areas

may be associated with lower temperatures (Fig. 6 and 7). However, the study has shown that the relationship is not linear (Fig. 8) and confirms conclusions from Yuan and Bauer (2007). Hence amount of vegetation is not the only factor affecting LST values. Consequently, NDVI alone cannot be used as a predictor of LST.

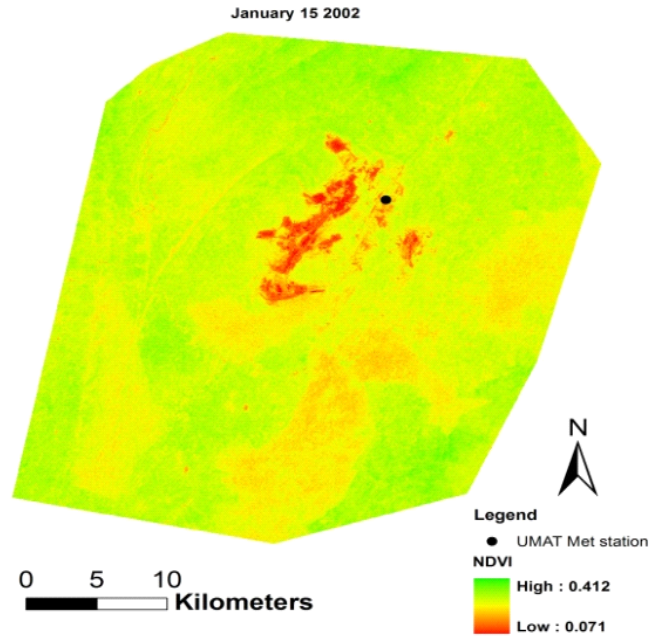


Fig. 5: NDVI map

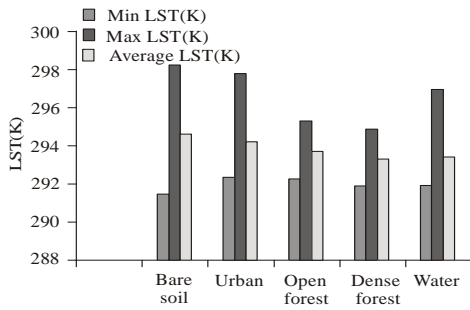


Fig. 6: LST and land covers

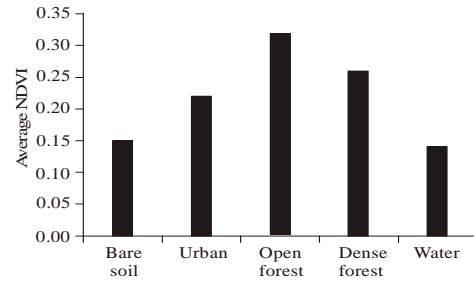


Fig. 7: NDVI and land covers

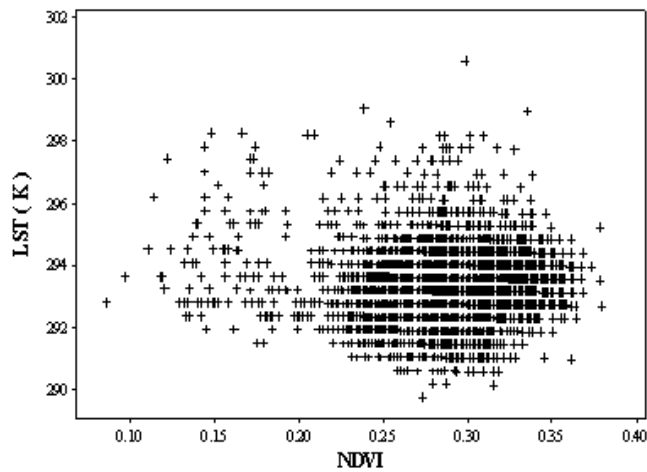


Fig. 8: LST and NDVI

In addition, the results indicate accurate modeling of LST. The average modeled LST was 293.38 Kelvin. Also the modeled LST at the UMaT Meteorological station was 298.60 Kelvin. This agrees with the average air temperature of 298.30 Kelvin recorded at the same station on January 15 2002. The accuracy is a confirmation of the study by Yuan and Bauer (2007). The results are indication of the potential in mapping LST operationally using optical satellite images in the study area without much error. However, there are a number of problems associated with using remote sensing for mapping LST in the tropics. Firstly, though there are a plethora of freely available images over the tropics, cloud cover often limits their use.

Also the temporal and spatial resolutions of the satellite images often possess many challenges. A dynamic phenomenon such as temperature needs preferably several images per day in order to map the variation of heat at different times of the day. For instance the image used in this study is from the Landsat 7 ETM+, a sensor with 16 day revisit time. Though the LST map produced has a high spatial resolution; it is only a snap shot of temperature at a point in time, in this case 10:10 GMT. To explore the temporal dynamics of temperature, time series high resolution images are required. Time series images would ensure that the temperature is mapped over a long period of time. In this way the data produced can be used to determine whether temperatures are actually changing or they are only showing seasonal variability. This study was therefore to confirm the possibility of operational mapping of LST using optical satellite remote sensing in humid tropical areas to complement traditional field measurements. Often it is not possible to install adequate number of climate stations to ensure complete coverage especially when funds are limited. The satellite methods are therefore necessary to generate information to manage the environment effectively. Remotely sensed methods ensure that LST is estimated at every point within the study area. The methods also allow all effects of the environment, for example topography, vegetation type, height and density etc to be accounted for.

Finally, LST maps produced in this study indicates the existence of an urban heat island in the Tarkwa area. It can be observed from Fig. 4 that LST of the urban and bare soils are higher than those of the vegetated areas. The average differences ranged between 0.87 Kelvin and 1.31 Kelvin while the maximum differences were between 2.90 Kelvin and 2.95 Kelvin. Also the villages surrounding the Tarkwa township show marked differences in temperature compared with the non-inhabited areas. Accordingly, when vegetated areas are converted into urban; there will be building up of heat since most of the surfaces become impervious and non-evaporative. Therefore, uncontrolled land use changes can intensify the urban heat island effect in Tarkwa.

## CONCLUSION

Remote sensing has been used successfully to detect urban heat island effect in the Tarkwa area using Landsat 7 ETM+ image. The Landsat 7 ETM+ sensor can therefore be used in operational mapping of LST for climate studies, vegetation and environmental monitoring in the humid regions of Ghana. This further confirms the important role Earth observation and geo-information techniques can play in effective management of the environment especially as the global land cover and climate continues to change.

## ACKNOWLEDGMENT

The authors wish to thank the Meteorological Station of the University of Mines and Technology (UMaT), Tarkwa, Ghana, for providing part of the data used in the study. Many thanks also go to the anonymous reviewers whose comments helped in fine tuning the manuscript.

## REFERENCES

- Coppin, E., I. Jonckheere, K. Nackaerts and B. Muys, 2004. Digital change detection methods in ecosystem monitoring: A review. *Int. J. Remote Sens.*, 25(9):1565-1596.
- Gluch, R., D.A. Quattrochi and J.C. Luvall, 2006. A multi-scale approach to urban thermal analysis. *Remote Sens. Environ.*, 104: 123-132.
- Gratton, D.J., P.J. Howarth and D.J. Marceau, 1993. Using Landsat-5 thematic mapper and digital elevation data to determine the net radiation field of a mountain glacier. *Remote Sens. Environ.*, 43: 315-331.
- Jensen, J.R., 2000. *Remote sensing of the environment: An earth resource perspective*. Prentice-Hall, New Jersey, pp: 181-243, 333-529.
- Kato, S. and Y. Yamaguchi, 2005. Analysis of urban heat-island effect using ASTER and ETM+ Data: Separation of anthropogenic heat discharge and natural heat radiation from sensible heat flux. *Remote Sensing Environment*, 99: 44-54.
- Kerle, N., L.L.F. Janssen and G.C. Huurneman, 2004. *Principles of Remote Sensing*. 3rd Edn., Enschede: ITC Educational Textbook Series, Netherlands, pp:212.
- Lillesand, T.M. and R.W. Kiefer, 1994. *Remote Sensing and Image Interpretation*, John Wiley & Sons, Chichester.
- Lunetta, R.S. and C.D. Elvidge, 1999. *Remote Sensing Change Detection, Environmental Monitoring Methods and Applications*. Taylor and Francis, London.

- Small, C., 2006. Comparative analysis of urban reflectance and surface temperature, *Remote Sensing Environment*, 104: 168-189.
- Sobrino, J.A., J.C. Jimenez-Munoz and L. Paolini, 2004. Land surface temperature retrieval from LANDSAT TM 5, *Remote Sens. Environ.*, 90: 434-440.
- Yuan, F. and M.E. Bauer, 2007. Comparison of impervious surface area and normalized difference vegetation index as indicators of surface urban heat island effects in Landsat imagery. *Remote Sens. Environ.*, 106: 375-386.